Journal of Materials Chemistry A

Accepted Manuscript

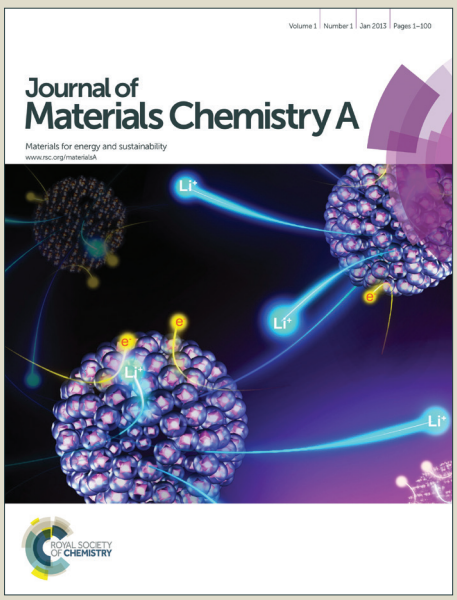

ROYAL SOCIETY OF CHEMISTRY

www.rsc.org/materialsA

Journal Name

RSCPublishing

ARTICLE

Graft octa-sulfonated poly(arylene ether) for high performance proton exchange membrane

Cite this: DOI: 10.1039/xoxxoooooox

Sinan Feng, Guibin Wang, Haibo Zhang, Jinhui Pang*

Received ooth January 2012,
Accepted ooth January 2012

DOI: 10.1039/xoxxoooooox

www.rsc.org/

A series of octa-sulfonated poly(arylene ether)s were prepared via a low-temperature grafting reaction and subsequent postsulfonation. The rigid backbone with high molecular weight conduces to a better integrity of hydrophobic domain. And the grafting ionic clusters are expected to promote the appearance of phase separation. These membranes with ion exchange capacity (IEC) values ranging from 1.19 to 1.90 meq. g^{-1} exhibited excellent dimensional stability, mechanical properties and oxidative stability. The membrane with higher IEC (>1.4 meq. g^{-1}) exhibited adequate conductivity (>100 mS cm^{-1}) in water at 80 °C. Furthermore, the membrane with IEC=1.90 meq. g^{-1} exhibited comparable conductivity to Nafion 117 under various humidity. In addition, SAXS profiles confirmed well-defined phase-separated morphology of SPAE-x. DMFC single cell performance demonstrate SPAE-*x* are good candidates for proton exchange membranes in fuel cell applications.

Introduction

The proton exchange membrane fuel cell (PEMFC) has been widely investigated as an automotive, stationary, and portable power source.[1-6] Proton exchange membrane (PEM) acts as an essential part of the fuel cell, which transfers protons from the anode to the cathode as well as serves as a barrier to fuel crossover between the electrodes. Perfluorosulfonic acid (PFSA) ionomers, represented by Nafion, are widely employed in conventional PEM materials application.[5, 7] Owing to the well-tailored structure constructed from poly(tetrafluoroethylene)-like hydrophobic backbones and hydrophilic perfluorosulfonic acid side chains, they own excellent chemical stability and high conductivity that meet the demands for PEM. Despite the advantages, PFSA membranes also face many issues to be worked out. At elevated temperature (>80 °C), they suffer from loss of mechanical properties and conductivity resulting in poor performance of PEM. Additionally, the complexity and high cost in the manufacture procedure of PFSA also hinder its development.

Sulfonated hydrocarbon polymers, such as sulfonated poly(arylene ether) (SPAE),[8-15] are regarded as the most promising alternatives of Nafion because of their excellent mechanical properties and low cost.[3-6, 16-18] SPAEs as versatile ionomer in PEM application have been comprehensively studied for recent years. However, conventional random SPAE copolymers suffered from excessive water swelling and insufficient conductivity, due to the ambiguously phase-separated microstructures and less acidic sulfonic acid groups.[11, 16, 19, 20] Hence, many arduous efforts are made to exploit types of SPAE with desired dimensional stability and enhanced conductivity for PEM. Among these strategies, adjusting the density of sulfonic acid groups seems an effective one. The concentrated sulfonic acid groups promote longer hydrophobic segment and cluster-like hydrophilic domain. Hay *et al.*[9] reported poly(arylene ether) with densely sulfonic acid groups on the end groups, and the polymers showed desirable conductivity due to the significantly phase-separated internal morphology. The strategy in their research worked, while the molecular weight of the ionomer was restricted due to the insufficient sulfonic acid end groups, which means it's hard to make a compromise between excellent mechanical properties and sufficient conductivity. Further, Ueda *et al.*[10] presented PES with localized sulfonic acid groups along the main chains accomplished by copolymerization with a tailored diphenol monomer with dense phenyl. The ion exchange capacity (IEC) values of the ionomers could be readily controlled by adjusting the content of the tailored monomer in total diphenol monomer. These PESs owned efficient proton conduction in a wide range of 30–95% RH at 80 °C, which were comparable with that of Nafion 117. However, the localized sulfonic acid groups distributed closely along the backbone and their mobility were reduced. And ionomer with higher IEC value (2.03 meq. g^{-1}) owned undesired water management that may result in loss of mechanical properties and durability. It's assumed that the polymers with insufficient molecular weight cannot afford desired dimensional stability. Pang *et al.*[21] demonstrated fluorinated PAEK with tetra-sulfonated side chains owning enhanced effective proton mobility and better dimensional stability. While under reduced RH, the membranes showed

much lower conductivity than Nafion 117. Additionally, the thermal and oxidative instability of aliphatic side chains is also a potential issue that hinders its application. Recently, we presented a series of PAE with penta-sulfonated pendent groups (SP-x) by adjusting the position of sulfonic acid groups.[22] Concentrated sulfonic acid groups apart from backbone facilitated the formation of phase-separated nanostructure and enhanced the integrity of the hydrophobic domain. SP-x polymer showed excellent mechanical properties, moderate water swelling and high conductivity comparable to Nafion 117. However, the tailored monomers with dense phenyl are supposed to barely afford sufficient reactivity in copolymerization due to the steric hindrance effect. With higher content of this monomer, the anticipated sulfonated polymer exhibited higher IEC values but a loss in molecular weight. Eventually, higher water uptake with declined mechanical properties lead to a poor performance in PEM application. SP-x with higher IEC value (>1.5 meq. g^{-1}) exhibited a dramatic increase in water swelling. Hence, the dilemma between dimensional stability and conductivity still exist, and we need to exploit a strategy to disengage it.

Herein, our research presents a strategy for preparing concentrated SPAE with enhanced conductivity and excellent mechanical stability. Briefly, the octa-sulfonated PAEs were prepared via a low-temperature grafting reaction and subsequent postsulfonation. Initially, a hydrophobic polymer precursor with grafting capability was obtained with high molecular weight. Then grafting reaction proceeded between the precursor and a tailored monomer at a lower temperature to give PAE polymer. The anticipated densely sulfonated polymer was obtained via a mild sulfonation of PAE polymer. Combining tough hydrophobic backbone and grafting ionic cluster, the sulfonated polymers are expected to own excellent dimensional stability and better phase-separation.

Experimental

Materials

2,6-Dimethoxynaphthalene (Phentex Corporation, Beijing), 4-fluorobenzoyl chloride (Jiangsu Haixiang Chemical Industry Co, Ltd), hexafluorobenzene (TCI) 4-triphenylmethylphenol (Alfa aesar) were used without further purification. 4,4'-Dihydroxydiphenylsulfone (DHDPS), 4,4'-difluorobenzophenone (DFB), chlorosulfonic acid, anhydrous $ZnCl_2$ and anhydrous K_2CO_3 were purchased from Sinopharm Chemical Reagent Co., Ltd. *N*-methyl pyrrolidone (NMP), *N*,*N*-dimethylacetamide (DMAc) and boron tribromide were purchased from Aladdin Reagent.

1,5-Bis(4-fluorobenzoyl)-2,6-dimethoxynaphthalene (a)

1,5-Bis(4-fluorobenzoyl)-2,6-dimethoxynaphthalene (**a**) was synthesized according to a procedure previous presented.[23] Mp: 260 °C. ^{1}H NMR (300 MHz, $CDCl_3$, δ): 7.91–7.87 (m, 4H), 7.64–7.62 (d, 2H), 7.28–7.26 (d, 2H), 7.13–7.09 (t, 4H), 3.79 (s, 6H). MALDI-TOF: m/z (%) 432 (100).

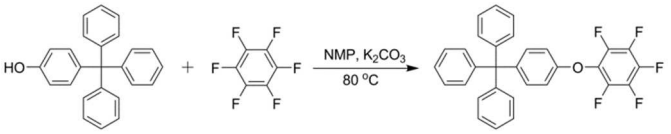

Scheme 1. Synthesis of monomer b.

4-Triphenylmethyl-pentafluorodiphenyl ether (b)

To a three-neck round-bottom flask equipped with a magnetic stirrer, an argon inlet/outlet, a Dean-Stark trap and a condenser, were added 4-triphenylmethylphenol (3.3643 g, 10 mmol), anhydrous K_2CO_3 (2.0732 g, 15 mmol), NMP (25 mL) and toluene (10 mL). The solution was reflux at 150 °C for 3 h to complete the azeotropic dehydration process, and then cooled to room temperature. Afterwards, hexafluorobenzene (11.1636 g, 60 mmol) was added into the solution and the mixture was heated at 80 °C for 12 h. And the argon purge was stopped considering the low boiling point (ca. 80 °C) of hexafluorobenzene. The mixture was poured into deionized water to precipitate the product. The precipitate was collected and washed with deionized water and hot isopropanol several times to obtain **b**. mp: 203 °C. ^{1}H NMR (300 MHz, $CDCl_3$, δ): 7.40–7.10 (m, 17H), 6.85–6.80 (d, 2H). ^{19}F NMR (470 MHz, $CDCl_3$, δ): −153.7 (d, $2F_1$), −159.9 (t, F_3), −162.1 (t, $2F_2$). MALDI-TOF: m/z (%) 501.9 (100).

Synthesis of poly(arylene ether)s containing methoxy groups (MPAE-x)

As follows: DHDPS (1.5016 g, 6 mmol), DFB (1.1128 g, 5.1 mmol), **a** (0.3892 g, 0.9 mmol), anhydrous K_2CO_3 (0.9122 g, 6.6 mmol), NMP (9 mL) and toluene (3 mL) were added into a three-neck round-bottom flask equipped with a mechanical stirrer, an argon inlet/outlet, a Dean-Stark trap and a condenser. The mixture was heated to reflux for 3 h to sufficiently dehydrate. Then the temperature was raised to 180 °C and the polymerization reaction proceeded smoothly for 6 h. The viscous mixture was poured into deionized water and the fibrous polymer was obtained. Washed with deionized water and isopropanol 5 times and dried in vacuo at 100 °C for 12 h, PAE-15 was obtained (94%).

Synthesis of poly(arylene ether)s precursor containing hydroxyl groups (HPAE-x)

MPAE-15 polymer (2 g) 1.3mmol was dissolved in methylene chloride (40 mL) and cooled to 0 °C by an ice bath. Then BBr_3 (0.6 mL) was mixed with methylene chloride (6 mL) and dropwise added into the polymer solution. The mixture was stirred for 8 h and then poured into deionized water. The resulting polymer was washed with deionized water and isopropanol 5 times, and then dried in vacuo at 60 °C for 24 h.

Grafting reaction of HPAE-x with monomer b

The grafting reaction was conducted as follows: 1 g of HPAE-15 (containing 0.66 mmol hydroxyl group), anhydrous K_2CO_3 (0.1368g, 0.99 mmol), NMP (10 mL) and cyclohexane (5 mL)

were charged into a three-neck round-bottom flask equipped with a mechanical stirrer, an argon inlet/outlet, a Dean-Stark trap and a condenser. The mixture dehydrated at 110 °C for 3 h and residual cyclohexane was removed afterwards. Then the mixture was cooled down below 50 °C and monomer b (0.4974 g, 0.99 mmol) was added. The mixture was heated to 80 °C and kept for 12 h. After cooled to room temperature, the mixture was poured into water to give fibrous polymer. Washed with deionized water and isopropanol 5 times and dried in vacuo at 100 °C for 12 h, PAE-*x* polymer was obtained.

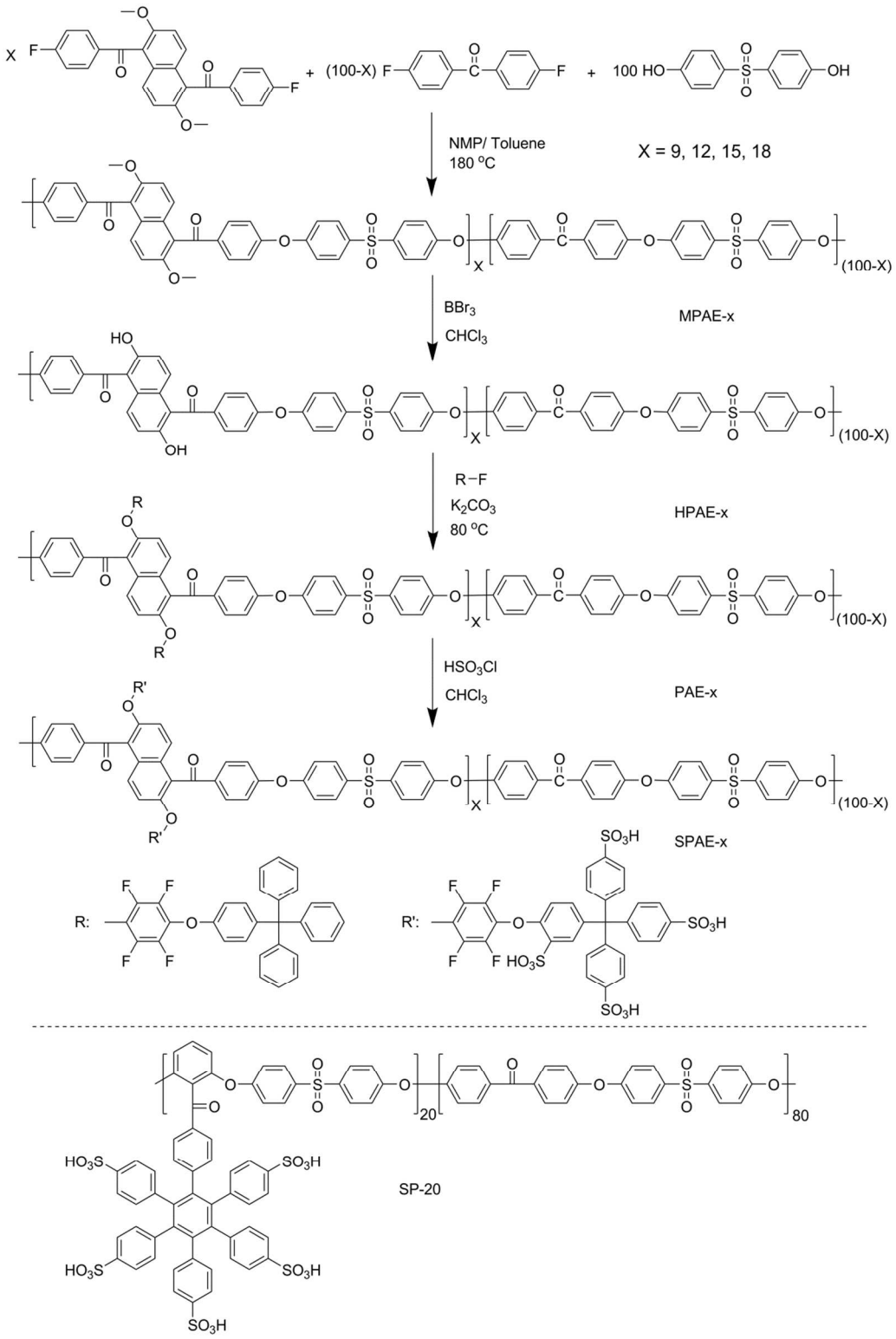

Scheme 2. Synthesis of SPAE-*x* with octa-sulfonated pendant groups. The structure of formerly reported penta-sulfonated SP-20 is included as a comparison.

Sulfonation of PAE-*x*

A typical sulfonation: PAE-15 polymer (1 g) was dissolved in methylene chloride (30 mL) and the solution was filtered through a 0.45 μm syringe filter. Then the polymer solution was placed in a round-bottom flask equipped with a magnetic stirrer and a $CaCl_2$ drying tube. After the solution cooled to 0–5 ^oC by an ice bath, 10.4 mL of 1 M chlorosulfonic acid solution in methylene chloride was dropwise added with vigorous stirring. The reaction mixture was stirred for 1 h and the product completely precipitated out of the solution. Then the supernatant was decanted and the precipitate was washed with hexane and then deionized water. The sulfonated polymer was dried in vacuo at 120 ^oC for 12 h to obtain SPAE-15.

Membrane preparation

Sulfonated polymer SPAE-*x* was dissolved in DMAc to form a clear polymer solution (8 wt%). Then, the solution was filtered through a 0.45 μm syringe filter and poured onto a clean glass plate, then carefully dried at 60 ^oC for 12 h and in vacuo at 100 ^oC for 24 h. The membranes were obtained after the solvent evaporation process. The acidification of the membranes was carried out by immersion in 1 M H_2SO_4 solution at 80 ^oC for 4 h and then washed with boiling water 5 times to remove residual acid. The membranes in their acid form were stored in deionized water for further investigation.

Instruments

The structure of monomer and polymers were characterized by ^1H NMR (Varian mercury 300 MHz) and ^{19}F NMR (Bruker Avance III 470 MHz). Fourier transform infrared (FTIR) spectra were measured on a Bruker Vector 22 FT-IR spectrometer. The reduced viscosities of polymers were determined by using an Ubbelohde viscometer with a 0.5 g dL^{-1} NMP solution at 25 ^oC.

Thermal analysis

Thermogravimetric analysis (TGA) of the polymers was carried out on a Perkin Elmer Pyris 1 thermal analyzer system with a heating rate of 10 ^oC min^{-1} from 100 ^oC to 800 ^oC under N_2 and air.

Ion exchange capacity

The ion exchange capacity (IEC) values of the membranes were evaluated by titration. The membranes were dried under vacuum and the weights were recorded. Then the membranes were immersed in 2 M NaCl solution for 72 h. The obtained solutions were titrated against a 0.05 M NaOH solution, with phenolphthalein as the indicator. The IEC (meq. g^{-1}) values were calculated from the titration results.

The volumetric IEC (IEC_v) values were defined as moles of $-SO_3H$ *vesus* dry/wet membrane volume:

$$IEC_v = \frac{IEC}{\frac{1}{\rho_p} + \frac{0.01WU}{\rho_w}}$$

where WU (%) was the water uptake of the membranes, ρ_p (g cm^{-3}) and ρ_w (g cm^{-3}) are the density of polymers and water, respectively.

Water uptake and swelling ratio

The membrane samples were dried under vacuum at 120 ^oC overnight prior to the measurement. After measuring the lengths and weights of the dry membranes, the samples were immersed in deionized water to reach equilibrium at the desired temperature. Then the lengths and weights of wet membranes were also measured. The water uptake (WU) was calculated as

$$WU = \frac{W_{wet} - W_{dry}}{W_{dry}} \times 100\%$$

where W_{dry} (g) and W_{wet} (g) are the weights of dry and corresponding water-swollen films, respectively. The percentage of length gain to original length was taken as the swelling ratio.

Proton conductivity

Impedance of hydrated membranes was performed on a frequency response analyzer/potentiostat (Princeton Applied Research PARSTAT 2273, EG&GPARC, Princeton, NJ) from 0.1 Hz to 100 kHz with 10 mV AC perturbation and 0.0 V DC rest voltage. The measurements were carried out with the cells immersed in constant-temperature water or under constant-humidity conditions, and the proton conductivity was determined by:

$$\sigma = \frac{L}{RA}$$

where σ (S cm^{-1}) is the proton conductivity, L (cm) is the distance between the electrodes used to measure the potential, R (Ω) is the membrane resistance, and A (cm^2) is the effective area.

Methanol permeability

The methanol permeability test of the membranes was conducted as described in earlier report.[8, 22] The methanol concentration was measured by a gas chromatography equipped with a thermal conductivity detector (Shimadzu, GC-2010A, Tokyo, Japan). The methanol permeability was calculated by the following equation:

$$c_B(t) = \frac{A}{V_B}\frac{DK}{L}c_A(t-t_0)$$

where V_B (in mL) is the volume of the receptor reservoirs, and A (in cm^2) and L (in cm) are the effective area and the thickness of the membrane, respectively. c_A and c_B (in mol L^{-1}) are the methanol concentration in the feed and in the receptor, respectively. DK (in cm^2 s^{-1}) represents the methanol permeability.

Membrane Electrode Assembly (MEA) and Single Cell Test

Pt/Ru black and 50% Pt/C were used for the anode and cathode respectively. The catalyst loading was 4 mg cm^{-2} for both the anode and the cathode and the effective electrode area of the single cell was 9 cm^2. The polarization curves of the passive

DMFCs were obtained on an Arbin FCTS system (Arbin Instrument Inc. USA). 2 M methanol aqueous solution was fed to the anode at a flow rate of 5 mL min^{-1} and oxygen was supplied to the cathode at 0.5 L min^{-1}.

Small Angel X-Ray Scattering

Prior to the test, a certain size of membrane sample was immersed in a 1 wt % lead acetate solution for 48 h to obtain the strained membrane. Small-angle X-Ray scattering (SAXS) experiments of the hydrated membrane samples were performed on a SAXSess mc^2 system (Anton Paar, Austria) equipped with a Mythen 1K CCD detector (Dectris, Switzerland). CuK_α radiation with a wavelength of $\lambda = 1.524$ Å was provided by a General Electric ID 3003 X-ray generator operating at 40 kV and 50 mA. The wave vector (q) was calculated according to:

$$q = \frac{4\pi \sin\theta}{\lambda}$$

where θ is the scattering angle. The characteristic separation length (d), i.e. the Bragg spacing, was calculated as:

$$d = \frac{2\pi}{q}$$

Oxidative stability

Typically, the accelerated oxidative stability test for sulfonated polymers is carried out by using Fenton's reagent (3% H_2O_2 containing 2 ppm Fe^{2+}). The membrane samples of SPAE-x were soaked in Fenton's reagent at 80 °C for 1 h, and the residual weight was recorded.

Mechanical properties

The mechanical properties of the dry membranes were measured on a AG-I 20kN Universal Tester (SHIMADZU, Japan) at room temperature and 30% RH. The tensile test was performed at a strain rate of 2 mm min^{-1}. The membranes were cut into a dumbbell shape and reached equilibrium prior to the measurement.

Results and discussion

Grafting monomer

Highly reactive monomer **b** was prepared via K_2CO_3-mediated nucleophilic aromatic substitution reaction as shown in Scheme 1. Hexafluorobenzene (HFB) was usually used in the synthesis of multiblock polymer as a coupling reagent of hydroxyl-terminated oligomers.[24-29] Attributed to the high reactivity of HFB, the coupling reaction could be conducted at a lower temperature. In this study, 4-triphenylmethylphenol was functionalized with HFB to give a highly reactive fluoride monomer **b** so that the subsequent grafting reaction could readily proceed. In order to obtain the target product, the reaction was conducted at a lower temperature (80 °C) and a fivefold excess of HFB was used. The structure of monomer was determined by ^{1}H NMR and ^{19}F NMR. In the ^{19}F NMR spectrum of monomer **b** (Figure 1), the signal from HFB at 164 ppm disappeared and 3 distinct signals were assigned to the fluorine atom from pentafluorophenyl. This demonstrated the desired highly reactive monomer **b** was obtained via a low–temperature nucleophilic substitution reaction.

Synthesis of poly(arylene ether)s precursor containing hydroxyl groups (HPAE-*x*)

1,5-bis(4-fluoro)benzoyl-2,6-dimethoxynaphthalene (**a**) was synthesized readily from 2,6-dimethoxynaphthalene and 4-fluorobenzoyl chloride by $ZnCl_2$-catalyzed Friedel-Crafts reaction as described in ref. 23. Towards the subsequent reaction, the dimethoxy groups can be converted to dihydroxyl owning grafting capability. Methoxy-containing poly(arylene ether) precursor MPAE-*x* (where "*x*" is the molar percentage of monomer **a** in the feed) was obtained by polycondensation of DHDPS, DFB and difunctional monomer **a**, as shown in Scheme 2. The polymerization reaction was conducted at 180 °C for 6 h and viscous polymer solution was obtained. With activated fluorine atoms, monomer **a** exhibited adequate reactivity in polymerization as expected. The obtained precursor MPAE-*x* showed good solubility in conventional solvents such as methylene chloride, DMAc and NMP. The chemical structure of MPAE-15 was characterized by ^{1}H NMR, the signal from methoxy group appeared at 3.72 ppm and all signals were well assigned as illustrated in Figure 2. To prepare HPAE-*x* containing hydroxyl groups, the demethylation reaction of MPAE-*x* was conducted by using BBr_3 known as a regiospecific demethylating reagent. The ^{1}H NMR spectrum of HPAE-15 confirmed complete demethylation occurred, since the signal from methoxy group at 3.72 ppm faded and the signal from hydroxyl group at 9.90 ppm appeared. Hence, this conversion of methoxy groups to hydroxyl groups endowed HPAE-*x* with grafting capability.

Grafting reaction

PAE-*x* was prepared via a grafting reaction between HPAE-*x* and monomer **b**, and this reaction was conducted at a low temperature attributed to the high reactive monomer with pentafluorophenyl group. The reaction proceeded smoothly and no crosslinking reaction was observed. Further, the lower temperature of this reaction gave rise to a minimum of ether-ether interchange reaction and desired grafting polymer.[24, 28, 29] The ^{1}H NMR spectrum of PAE-15 reveals the complete disappearance of signal from hydroxyl groups at 9.90 ppm and signals from monomer **b** appeared in the range of 7.05–7.25 ppm overlapping with that of protons (H_7, H_2, H_3, H_5, H_8) from polymer backbone. This implies that all the hydroxyl groups reacted with pentafluorophenyl groups. Further, in the ^{19}F NMR spectrum of PAE-15, the signals of F_2 and F_3 disappeared and the signal of F_1 shifted to 155 ppm. This confirms the fluorine atom on the para position of pentafluorophenyl participated in the grafting reaction as expected. The obtained PAE-*x* was readily dissolved in $CHCl_3$, DMAc and NMP. The viscosities of PAE-*x* were in the range of 0.58–0.65 dL g^{-1} which demonstrated grafting polymer with high molecular weight was obtained.

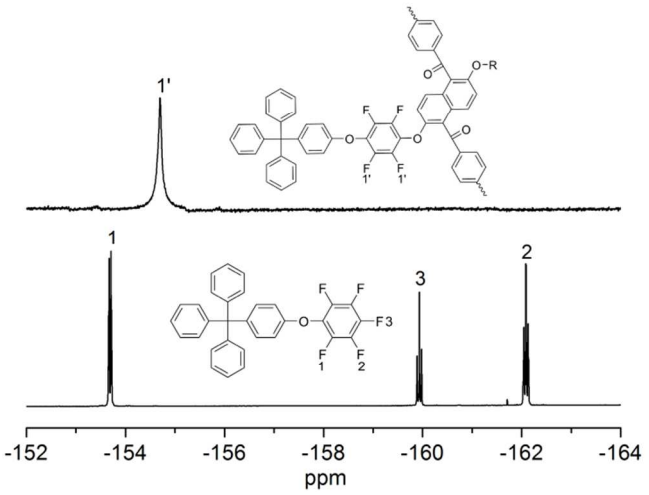

Figure 1. [19]F NMR spectra of monomer b and PAE-15

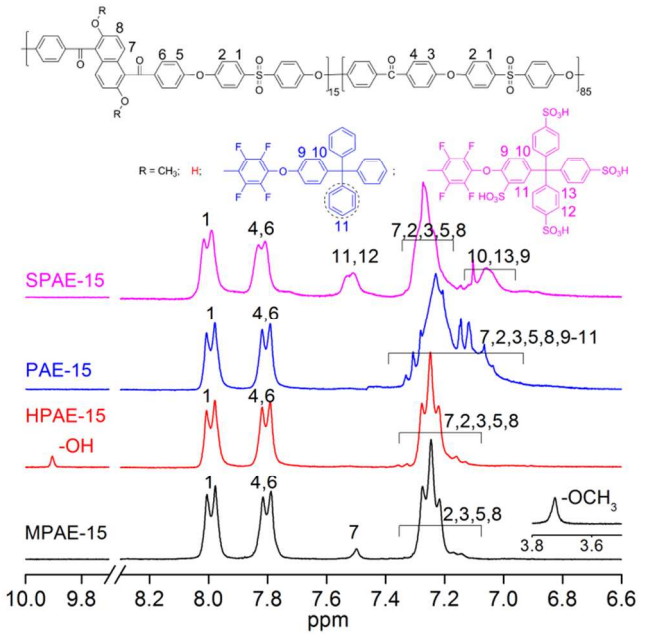

Figure 2. [1]H NMR spectra of MPAE-15, HPAE-15, PAE-15 and SPAE-15

Sulfonation

Sulfonation as an electrophilic substitution reaction was utilized to introduce sulfonic acid groups into activated aromatic rings.[1, 3, 11] Herein, DFB and DHDPS with electron withdrawing groups (carbonyl or sulfone groups) were elected to build the hydrophobic backbone owing to the excellent stability through sulfonation. Hence, it was expected that the sulfonation of PAE-*x* would proceed on the dense phenyls of grafting pendant groups. For the choice of sulfonation agent, chlorosulfonic acid is considered as a milder one in comparison with concentrated H_2SO_4 and no cleavage of polymer occurred through sulfonation reaction. As noted in some earlier literature, the reaction time of sulfonation should be precisely controlled when using chlorosulfonic acid to avoid the formation of insoluble gel. In this work, the sulfonation of PAE-*x* proceeded at 0–5 °C for 1 h and the sulfonated polymer completely precipitated out the solution during this period. The obtained SPAE-*x* showed good solubility in DMAc, DMSO and NMP, and the viscosities of SPAE-*x* were in the range of 1.32–1.58 dL g^{-1}. This suggested that no cross-linking or cleavage occurred throughout the sulfonation reaction. The [1]H NMR spectrum of SPAE-15 is also included in Figure 2, the signals of H_{11} and H_{12} shifted to 7.5 ppm after sulfonation. Further, the characteristic IR absorption of the sulfonic acid group ($\nu_{S=O}$) and diphenylcarbonyl ($\nu_{C=O}$) were observed at 1036 and 1658 cm^{-1}, respectively. The degree of sulfonation was determined by the IEC value through acid-base titration. All above confirm that the postsulfonation proceeded successfully as we expected.

Thermal stability

To estimate the thermal stability of PAE-*x* and SPAE-*x*, the TGA was performed under a N_2 atmosphere. The 5% weight loss temperatures of SPAE-*x* are listed in Table 1. And the TGA curves of SPAE-*x* and PAE-9 are plotted in Figure 3. PAE-*x* exhibited excellent thermal stability and the 5% weight loss temperature were higher than 523 °C. The 5% weight loss temperatures of these sulfonated polymers were higher than 341 °C and showed a decline as IEC values increased. The dTG were applied to determine the detailed weight loss process. The polymers showed trace weight loss before 280 °C due to the interaction between sulfonic acid groups and residual solvent.[30] As temperature increased, SPAE-*x* exhibited a two-step degradation proceeded during the heating period. The degradation involves the thermolysis of sulfonic acid around 300–400 °C and the decomposition of polymer backbone. The dTG curves revealed the rate of the degradation correlated to the IEC values. And SPAE-18 exhibited 15.5% loss in weight during the first step, which is close to the theoretical value of 15.2% after cleavage of sulfonic acid. The decomposition of polymer backbone ceased when temperature was higher than 700 °C and the char yield of the polymers were higher than 50% attributed to their excellent thermal stability. The thermo-oxidative stability of SPAE-*x* were assessed by TGA analyses under air atmosphere and no weight loss were observed below 200 °C demonstrating excellent resistance to thermo-oxidation.

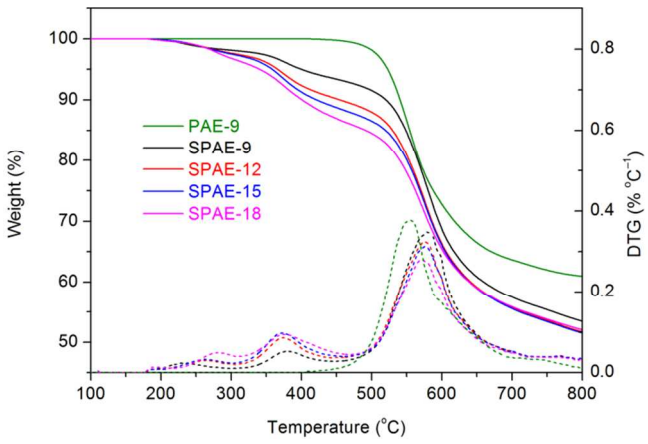

Figure 3. TGA and DTG curves of SPAE-*x* and PAE-9

Table 1. Some properties of the polymers

Polymer	IEC_w (meq. g^{-1})[a]	IEC_w (meq. g^{-1})[b]	η (dL g^{-1})[c]	$T_{d5\%}$ (°C)[d]	Char yield (%)[e]	Thickness of dry membrane	Oxidative stability (%)[f]	Tensile strength (MPa)	Elongation at break (%)
SPAE-9	1.22	1.19	1.32	390	53.5	56±3	98.6±0.8	44.4±4.2	139.9±5.4
SPAE-12	1.49	1.47	1.47	366	51.7	46±1	97.8±0.8	42.1±1.0	138.9±2.8
SPAE-15	1.72	1.67	1.51	352	51.5	50±2	96.0±0.7	33.0±3.8	119.6±9.1
SPAE-18	1.92	1.90	1.58	341	52.0	57±3	95.1±0.5	29.6±1.2	110.6±7.9

[a] Calculated value from the feed monomer ratio. [b] Calculated from acid–base titration. [c] Measured in NMP with 0.5 g dL^{-1} at 25 °C. [d] Measured under N_2 atmosphere. [e] Calculated from data at 800 °C under N_2 atmosphere. [f] Residual weight after immersing in Fenton's reagent at 80 °C for 1 h.

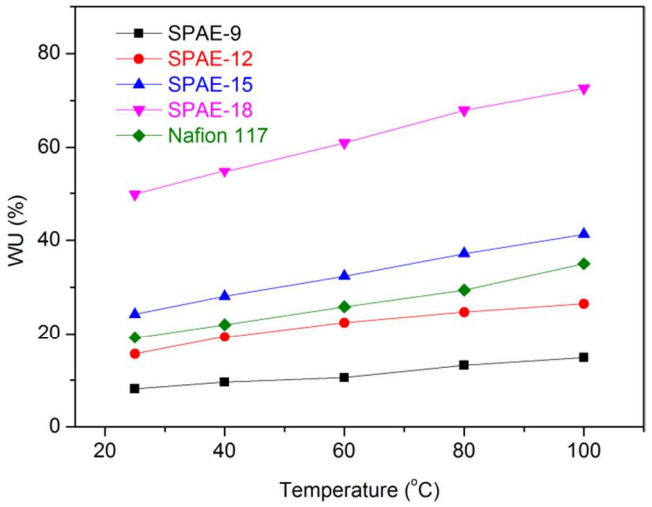

Figure 4. Water uptake of SPAE-x as a function of temperature

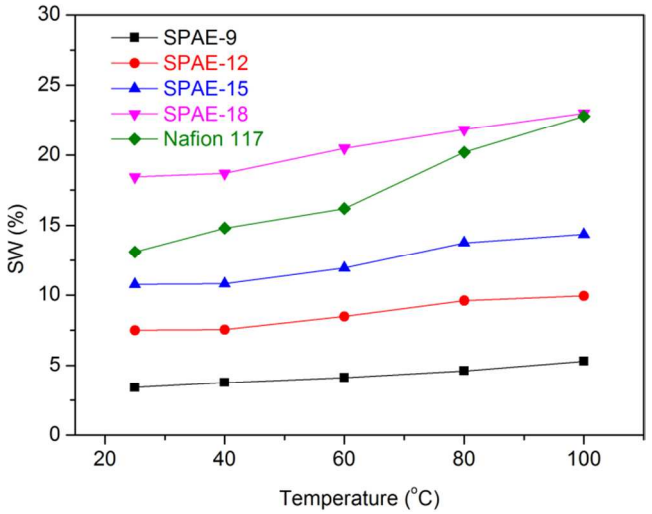

Figure 5. Swelling ratio of SPAE-*x* as a function of temperature

Water uptake and swelling ratio

Water, an essential component of PEMs, acts as a media for dissociation of sulfonic acid and proton transportation. As to the conventional sulfonated polymers, higher IEC value endows membrane with higher conductivity but results in excessive water uptake. Further, water-induced plasticization of the membrane may lead to a loss in the tensile strength. The densely sulfonated polymers are expected to own a better water management due to their longer hydrophobic segment and cluster-like hydrophilic domain. Herein, the water uptake (*WU*) and swelling ratio (*SW*) of SPAE-*x* was measured at various temperatures and the data were listed in Table 2. At 25 °C, the *WU*s of SPAE-*x* were in the range of 8.1–49.8% and the *SW*s were from 3.4% to 18.4%. As illustrated in Figure 4, the *WU* of SPAE-*x* increased with elevated temperature. At a certain temperature, the *WU* was closely relevant to the IEC value. The *SW* of SPAE-*x* (displayed in Figure 5) also exhibited a similar tendency with *WU*. At 25 °C, SPAE-18 showed the highest *WU* (49.8%) and *SW* (18.4%) in this series. When the temperature went to 80 °C, SPAE-18 was observed to have 36.3% increase in *WU* and 18.5% increase in *SW*. As to SP-20, the rate of increase in *WU* and *SW* were 53.4% and 61.2%, respectively. This phenomenon revealed that SPAE-*x* own less hydration-temperature dependence and have better water management than SP-20 even at a higher IEC level. Compared to Nafion 117, SPAE-18 possessed higher *WU* and comparable *SW*. This demonstrated that SPAE-18 have better dimensional stability even bonding with more water. Further, the higher *WU* was attributed to the higher IEC value of SPAE-18 and this may facilitate the dissociation of sulfonic acid and proton transportation.

Conductivity and methanol permeability

The proton conductivity of fully hydrated SPAE-*x* was measured at various temperatures. As listed in Table 2, conductivity of SPAE-*x* increased from 79 to 152 mS cm^{-1} at 80 °C which is higher than corresponding SP-x with the similar IEC value. Since SP-x owned higher water uptake and swelling ratio than SPAE-*x*, the excessive water diluted the acid concentration of membrane leading to a loss of conductivity. And IEC_v for each membrane was calculated to estimate the change of acid concentration inside the wet membranes at various state of water-swollen. As displayed in Figure 6, SPAE-18 and SP-20 showed dramatic decrease in IEC_v values once the membranes hydrated. While the IEC_v of SPAE-9 and SPAE-12 tended to decline smoothly as temperature increased, due to the lower water content.

Table 2. Water uptake, swelling ratio, conductivity and methanol permeability data of PAES-x

Polymer	Water uptake (%)[a]		Swelling ratio (%)[a]		σ (mS cm^{-1})[a]		E_a (kJ mol^{-1})	Methanol permeability (10^{-7} cm^2 s^{-1})
	20 °C	80 °C	20 °C	80 °C	20 °C	80 °C		
SPAE-9	8.1±0.2	13.1±0.2	3.4±0.1	4.6±0.1	44±2	79±4	9.04	0.98
SPAE-12	15.6±0.2	25.7±0.5	7.5±0.2	9.6±0.2	62±1	100±2	8.16	1.90
SPAE-15	24.3±0.6	37.2±1.1	10.8±0.2	13.8±0.2	80±3	130±5	7.68	2.77
SPAE-18	49.8±1.9	67.9±2.5	18.4±0.4	21.8±0.5	94±5	152±7	7.52	4.51
SP-20	30.5	46.8	14.7	23.7	55	122	11.63	3.79
Nafion 117	19.2	29.4	13.1	20.1	80	122	6.77	29.4

[a]Measured in fully hydrated state

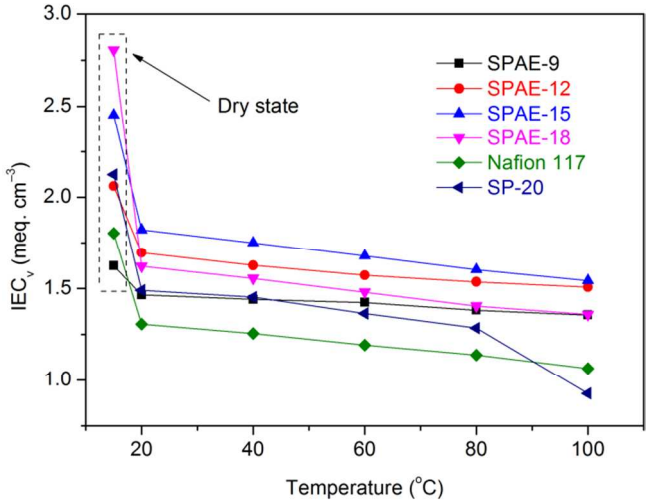

Figure 6. IEC$_v$ of SPAE-*x*, SP-20 and Nafion 117 as a function of temperature.

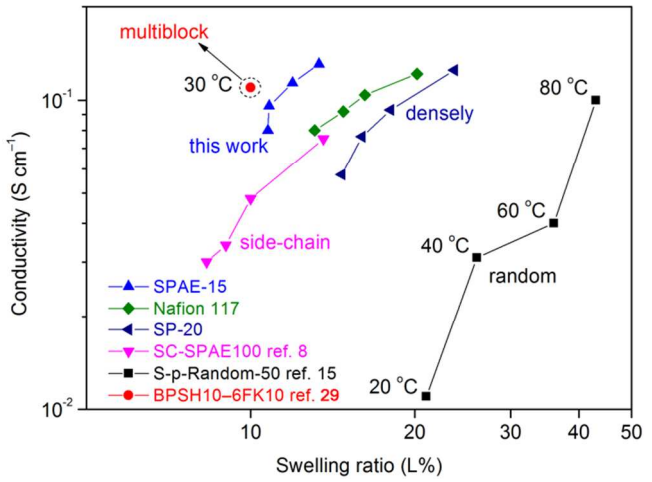

Figure 7. Proton conductivities and swelling ratio (L%) of different types of sulfonated polymers at various temperatures.

Figure 7 shows the relationship between swelling ratio (L%) and conductivity at various temperatures. S-p-Random-50 as a type of random sulfonated polymer exhibits insufficient conductivity at lower temperatures and undesired excessive swelling at 80 °C. Further, the dimensional stability and conductivity have been partially balanced in side-chain-type and densely sulfonated poly(arylene ether)s. In this work, SPAE-15 owns better dimensional stability and enhanced conductivity compared to the former types. As temperature increases, the swelling ratio of SPAE-15 varies in a small range (10%–14%) and the conductivity maintains the same level with that of Nafion 117. In addition, the similarity between SPAE-15 and BPSH10-6FK10 reveals the nature of micro-block structure in SPAE-15 which facilitates the formation of phase separation. And the detailed morphological characterization will be discussed later in this paper.

Figure 8 displayed Arrhenius plot of proton conductivities as a function of temperature. Compared to Nafion 117, SPAE-15 showed comparable conductivity but lower swelling ratio in the entire testing range. Further the highest proton conductivity of 185 mS cm^{-1}, was obtained from SPAE-18 with IEC of 1.90 meq. g^{-1} at 100 °C, which is higher than that of Nafion 117 measured under the same condition. The activation energy (E_a) for conductivity was calculated from the slope of the linear fit and listed in Table 2. Apparently, the E_a values of SPAE-*x* are lower than SP-20 and comparable with Nafion 117. With increasing IEC values, the E_a values slightly decreased from 9.04 to 7.52 kJ mol^{-1}. It's assumed that well phase-separation does favor to construct proton transportation channel and thus lower the E_a value.

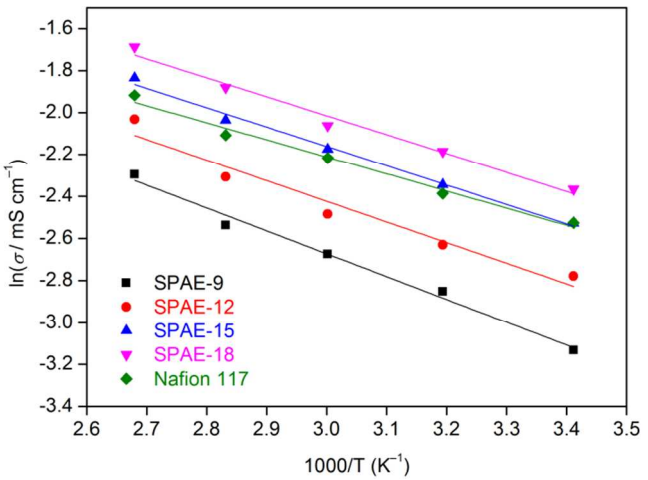

Figure 8. Arrhenius plot of proton conductivity (in water) as a function of temperature.

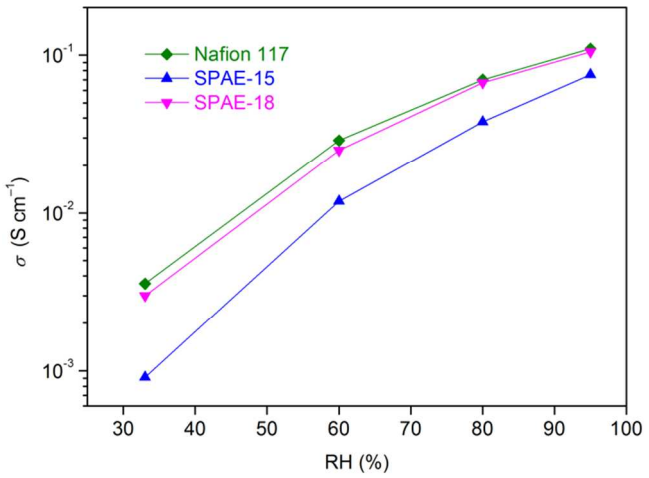

Figure 9. Proton conductivity of Nafion 117, SPAE-15 and SPAE-18 under different RH at 80 °C.

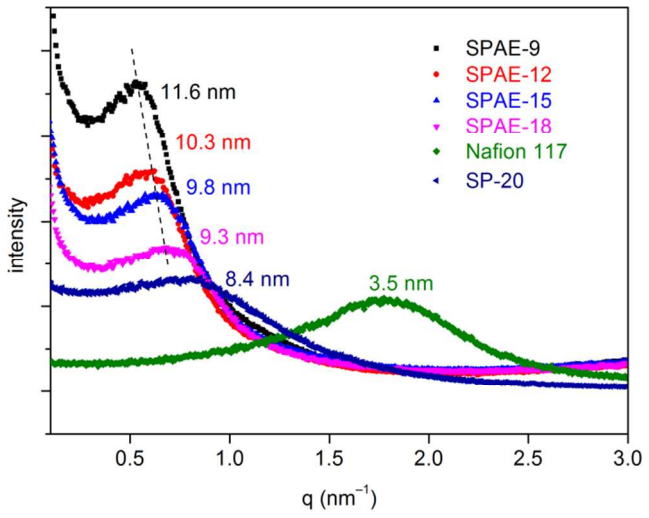

Figure 10. SAXS intensity profile of SPAE-*x* and Nafion 117

As shown in Figure 9, the proton conductivities of Nafion 117, SPAE-15 and SPAE-18 were measured at 80 °C in the range of 30–95% RH. Compared to Nafion 117, SPAE-18 exhibited comparable conductivity over the entire RH range. Even under reduced humidity (33% RH), SPAE-18 maintained adequate conductivity of 3 mS cm^{-1}. In addition, SPAE-15 showed slightly lower conductivity than SPAE-18 due to its insufficient IEC value. Hence, SPAE-18 exhibited improved proton conductivity and less conductivity-RH dependence, which may be explained by the formation of the well-defined phase separation.

The methanol permeability of SPAE-*x* was evaluated considering their potential application in direct methanol fuel cells (DMFC). The measurement was conducted at room temperature and 10 mol L^{-1} was employed. And the data are summarized in Table 2. The methanol permeability is closely relevant to the water behavior of the membranes since the wider ionic domain facilitate the diffusion of methanol. As IEC values ranging from 1.19 to 1.90 meq. g^{-1}, the methanol permeability of SPAE-*x* increased from 0.98 to 4.51 × 10^{-7} cm^2 s^{-1}, which are much lower than Nafion 117. Compared to SP-20, SPAE-12 with similar IEC value exhibited much lower permeability. Since SP-20 has higher water uptake and swelling ratio, the ionic domain within it expand excessively and methanol crossover occurs. Considering the higher IEC level, SPAE-18 owns moderate methanol permeability (4.51 × 10^{-7} cm^2 s^{-1}) of which is about one-sixth of Nafion 117. Indeed, SPAE-*x* exhibit low methanol permeability and could be promising materials for DMFC applications.

Morphology

SAXS experiment is widely used to investigate the nanostructure of ionomers. The morphological differences between Nafion membranes and conventionally sulfonated hydrocarbon aromatic membranes have previously been extensively discussed by Kreuer and Jannasch on the basis of SAXS data.[12, 17, 31-33] Further, concentrated sulfonated polymers are anticipated to have an enhanced phase separation owing to their longer hydrophobic segment and sulfonic acid clusters.[22, 34] In this work, the SAXS experiment of hydrated SPAE-*x* membranes were performed at room temperature in the q range of 0.02–5 nm^{-1}. As shown in Figure 10, all the sulfonated polymers display a distinct ionomer peak as well as Nafion 117. In addition, the ionomer peaks of SPAE-*x* are narrower and appear at lower q values, and these findings are consistent with Jannasch's work. The characteristic separation length of these ionomers were calculated and included in Figure 10. Obviously, SPAE-*x* owned larger *d* values than Nafion 117, suggesting more concentrated ionic domain within their membranes. Considering the flexible nature of polymer structure and pendant mono-functional group, Nafion is expected to form distributed ionic domain. In contrast, the longer hydrophobic segment and octa-sulfonic acid pendant of SPAE-*x* facilitates the concentration of ionic domain. Further, a correlation may exist between IEC and the d values of SPAE-*x*. As IEC values ranging from 1.19 to 1.90 meq. g^{-1}, the *d* values decrease from 11.6 nm for SPAE-9 to 9.3 nm for SPAE-18. Hence, the ionic domain possesses larger area in SPAE-*x* with higher IEC value. This is consistent with the result of water behavior and conductivity. At a comparable IEC level, SPAE-15 exhibits higher d value than SP-20 as illustrated in SAXS profiles. This reveals that longer hydrophobic segments induced increased characteristic separation length in SPAE-*x* polymers. In addition, longer hydrophobic segments do favor to enhance the dimensional stability which corresponds to the results of water swelling data.

Mechanical properties and oxidative stability

To evaluate the mechanical properties of SPAE-*x* polymers, the tensile testing of membranes were performed under low relative humidity (RH=30%) and the results are listed in Table 1. The tensile strength of SPAE-*x* was observed between 29.6 and 44.4 MPa, and the elongation at break was from 110.6% to 139.9%. In the stress-strain curves of SPAE-*x* (Figure 11), a decline of tensile strength was found as IEC value increased. It's assumed

that sulfonic acid groups inevitably alter the nature of the polymer backbone, and this made sulfonated polymers exhibit poorer tensile strength than the unsulfonated ones. Usually, SPAE membranes in dry state are very brittle and the elongations of them are lower than 30%. In contrast, SPAE-*x* performed well in ductility and owned elongation even at a higher IEC level (1.90 meq. g^{-1}).

The oxidative stability test, which indirectly shows PEM durability to free radical attack, was done by comparing the PEM weight changes after soaking in Fenton's reagent (3 wt% H_2O_2 containing 2 ppm Fe^{2+}) at 80 °C for 1 h and the result is summarized in Table 1. All the sulfonated polymers exhibited residual weight over 95% and their properties such as flexibility and transparency were maintained after the test. The tensile test was also performed to evaluate the mechanical properties of membranes after treatment with Fenton's reagent. The tensile strength of all the membranes maintained the original level (>90%) whereas the elongation at break decreased to some extent. SPAE-15 and SPAE-18 owning higher IEC level (>1.4 meq. g^{-1}) showed considerable loss (~50%) in elongation due to the degradation of sulfonic acid groups in hydrophilic domain.

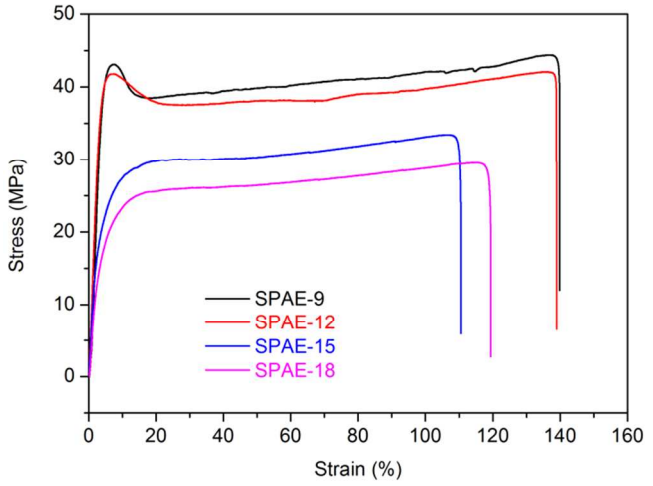

Figure 11. Stress-strain curves of SPAE-*x* at room temperature and 30% RH

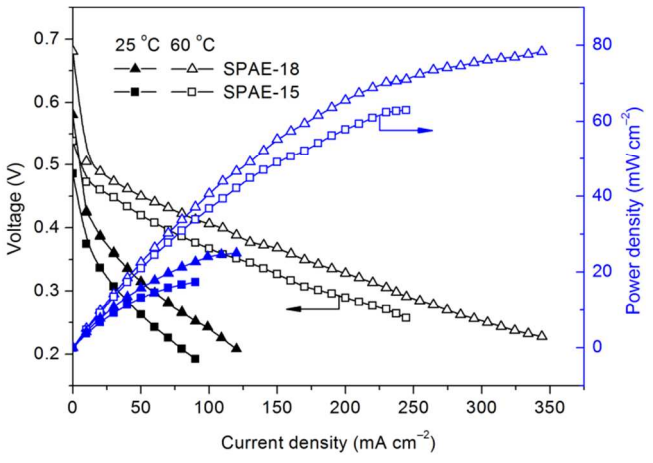

Figure 12. Single cell performance of SPAE-15 and SPAE-18 at 25 °C and 60 °C using 2 M methanol and O_2 as fuel and oxidant, respectively.

Single cell evaluation

To exactly demonstrate the practical application of SPAE-x in fuel cell systems, MEA with SPAE-15 and SPAE-18 were performed and evaluated via a single cell test of a DMFC. As shown in Figure 12, the polarization and power density curves were obtained. At a certain temperature, SPAE-18 exhibited better cell performance than SPAE-15 due to the higher proton conductivity. The maximum power density was 25 mW cm^{-2} and 78.3 mW cm^{-2} for SPAE-18 at 25 °C and 60 °C, respectively. The result demonstrate our membranes have good potential to be an alternative PEM for fuel cell applications.

Conclusion

A series of octa-sulfonated poly(arylene ether)s (SPAE-*x*) were prepared via a low-temperature grafting reaction and subsequent postsulfonation. The polymer backbone was obtained via a copolymerization of difunctional monomer, DHDPS and DFB. The grafting reaction proceeded at a lower temperature (80 °C) by using a highly reactive multi-phenyls monomer. The rigid backbone with high molecular weight conduces to a better integrity of hydrophobic domain. And the grafting ionic clusters are expected to promote the appearance of phase separation. Compared to our earlier work, these membranes exhibited enhanced dimensional stability and superior proton conductivity. SPAE-18 with IEC=1.90 meq. g^{-1} exhibited comparable conductivity (3 mS cm^{-1}) with Nafion 117 (3.6 mS cm^{-1}) even under reduce humidity (33% RH). In addition, SAXS profiles confirmed well-defined phase-separated morphology of SPAE-*x*. Additionally, the DMFC single cell performance demonstrated these octa-sulfonated polymers are promising candidate for PEM in fuel cell applications.

Acknowledgements

The authors would like to thank the China Natural Science Foundation (Grant no: 51103060), and the Science and Technology Development Plan of Jilin Province, China (no.: 20140309001GX).

Notes and references

Corresponding author: Jinhui Pang
E-mail: pangjinhui@jlu.edu.cn
Address: Key Laboratory of Super Engineering Plastic of Ministry of Education, Jilin University, Qianjin Street 2699, Changchun 130012, P.R. China

1. M. A. Hickner, H. Ghassemi, Y. S. Kim, B. R. Einsla and J. E. McGrath, *Chem. Rev.*, 2004, **104**, 4587-4612.
2. M. Winter and R. J. Brodd, *Chem. Rev.*, 2004, **104**, 4245-4270.
3. H. Zhang and P. K. Shen, *Chem. Rev.*, 2012, **112**, 2780-2832.
4. R. Devanathan, *Energy Environ. Sci.*, 2008, **1**, 101-119.
5. S. Bose, T. Kuila, T. X. H. Nguyen, N. H. Kim, K.-t. Lau and J. H. Lee, *Prog. Polym. Sci.*, 2011, **36**, 813-843.
6. C. H. Park, C. H. Lee, M. D. Guiver and Y. M. Lee, *Prog. Polym. Sci.*, 2011, **36**, 1443-1498.
7. K. A. Mauritz and R. B. Moore, *Chem. Rev.*, 2004, **104**, 4535-4586.
8. J. Pang, H. Zhang, X. Li and Z. Jiang, *Macromolecules*, 2007, **40**, 9435-9442.

9. S. Matsumura, A. R. Hlil, C. Lepiller, J. Gaudet, D. Guay and A. S. Hay, *Macromolecules*, 2008, **41**, 277-280.
10. K. Matsumoto, T. Higashihara and M. Ueda, *Macromolecules*, 2009, **42**, 1161-1166.
11. B. Liu, G. P. Robertson, D.-S. Kim, M. D. Guiver, W. Hu and Z. Jiang, *Macromolecules*, 2007, **40**, 1934-1944.
12. B. Lafitte and P. Jannasch, *Adv. Funct. Mater.*, 2007, **17**, 2823-2834.
13. K. Miyatake, Y. Chikashige, E. Higuchi and M. Watanabe, *J. Am. Chem. Soc.*, 2007, **129**, 3879-3887.
14. N. Li, C. Wang, S. Y. Lee, C. H. Park, Y. M. Lee and M. D. Guiver, *Angew. Chem.*, 2011, **123**, 9324-9327.
15. M. Guo, X. Li, L. Li, Y. Yu, Y. Song, B. Liu and Z. Jiang, *J. Membr. Sci.*, 2011, **380**, 171-180.
16. T. J. Peckham and S. Holdcroft, *Adv. Mater.*, 2010, **22**, 4667-4690.
17. K.-D. Kreuer, *Chem. Mater.*, 2014, **26**, 361-380.
18. N. Li and M. D. Guiver, *Macromolecules*, 2014, **47**, 2175-2198.
19. T. J. Peckham, J. Schmeisser, M. Rodgers and S. Holdcroft, *J. Mater. Chem.*, 2007, **17**, 3255-3268.
20. T. Higashihara, K. Matsumoto and M. Ueda, *Polymer*, 2009, **50**, 5341-5357.
21. J. H. Pang, S. N. Feng, Y. Y. Yu, H. B. Zhang and Z. H. Jiang, *Polym. Chem.*, 2014, **5**, 1477-1486.
22. J. Pang, K. Shen, D. Ren, S. Feng, Y. Wang and Z. Jiang, *J. Mater. Chem. A*, 2013, **1**, 1465-1474.
23. M. Zhu, X. Liu, B. J. Liu, Z. H. Jiang and T. Matsumoto, *Polym. Bull.*, 2011, **67**, 1761-1771.
24. K. Nakabayashi, K. Matsumoto and M. Ueda, *J. Polym. Sci., Part A: Polym. Chem.*, 2008, **46**, 3947-3957.
25. S. Takamuku and P. Jannasch, *Adv. Energy Mater.*, 2012, **2**, 129-140.
26. S. Takamuku and P. Jannasch, *Macromolecules*, 2012, **45**, 6538-6546.
27. H.-S. Lee, A. Roy, O. Lane, S. Dunn and J. E. McGrath, *Polymer*, 2008, **49**, 715-723.
28. G. Titvinidze, K.-D. Kreuer, M. Schuster, C. C. de Araujo, J. P. Melchior and W. H. Meyer, *Adv. Funct. Mater.*, 2012, **22**, 4456-4470.
29. H.-S. Lee, A. Roy, O. Lane, M. Lee and J. E. McGrath, *J. Polym. Sci., Part A: Polym. Chem.*, 2010, **48**, 214-222.
30. G. P. Robertson, S. D. Mikhailenko, K. Wang, P. Xing, M. D. Guiver and S. Kaliaguine, *J. Membr. Sci.*, 2003, **219**, 113-121.
31. K. D. Kreuer, *J. Membr. Sci.*, 2001, **185**, 29-39.
32. E. P. Jutemar and P. Jannasch, *J. Membr. Sci.*, 2010, **351**, 87-95.
33. X.-F. Li, F. P. V. Paoloni, E. A. Weiber, Z.-H. Jiang and P. Jannasch, *Macromolecules*, 2012, **45**, 1447-1459.
34. S. Feng, K. Shen, Y. Wang, J. Pang and Z. Jiang, *J. Power Sources*, 2013, **224**, 42-49.

Table of contents entry

Graft octa-sulfonated poly(arylene ether) for high performance proton exchange membrane

Sinan Feng, Guibin Wang, Haibo Zhang, Jinhui Pang*

A novel octa-sulfonated poly(arylene ether)s was combined with longer hydrophobic backbone and grafting ionic clusters, exhibited high proton conductivity and excellent dimensional stability.